Eccentric Dynamical Tides

Yubo Su[1], Dong Lai[1]
[1] *Cornell Center for Astrophysics and Planetary Science, Department of Astronomy, Cornell University, Ithaca, NY 14853, USA*

Accepted XXX. Received YYY; in original form ZZZ

ABSTRACT
Abstract

Key words: keywords

1 INTRODUCTION

In the course of their evolution, massive stellar binaries give rise to many astrophysical systems of interest including high mass x-ray binaries (HMXRBs) and compact object binaries (CITATION with evolutionary pathway). In general, the more massive star undergoes a supernova before its less massive companion, after which the binary consists of one massive star and one compact object in an eccentric orbit (MS-CO binary). In such a system, the evolution is dominated by the torque from the compact object on the massive star due to dynamical tides. While this tidal torque is now well understood for circular binaries (Kushnir et al. 2017), it has not been carefully studied for binaries with substantial eccentricities. The tidal evolution of such eccentric binaries sculpt the population of HMXRBs (CITE) as well as the population of compact object binaries (Vigna-Gómez et al. 2020).

The dissipation due to the dynamical tide in a massive star's envelope under the influence of a *circular* perturber is traditionally understood via Zahn's parameterized theory of dynamical tides (Zahn 1975). However, Zahn's theory relies on a dimensionless parameter E_2 reflecting the detailed stellar structure that varies over many orders of magnitudes for typical stars. In general, the value of E_2 is taken from empirical fits to simplified stellar models (Hurley et al. 2002; Vigna-Gómez et al. 2020). The introduction of this uncertain parameter E_2 is because the dynamical tidal torque arises due to excitation of internal gravity waves at the radiative convective boundary (RCB) (Goldreich & Nicholson 1989; Savonije & Papaloizou 1983), but Zahn's formula is evaluated at the *stellar* radius. Instead, it is possible re-express the tidal torque in terms of quantities evaluated at the RCB itself, for which dimensionless parameters are generally of order unity for a wide range of stars (Kushnir et al. 2017). However, Kushnir et al. (2017) only consider circular binaries.

To study the dynamical tide in eccentric binaries, it is natural to decompose the perturbing potential into Fourier harmonics, each of which is analogous to a perturber on a circular orbit (e.g. Storch & Lai 2013; Vick et al. 2017). While accurate, such decompositions are unwieldy to evaluate as the eccentricity increases, often requiring summing hundreds of terms and lending little intuition to the broad scalings of the tidal torque. In this work, we show that, for the circular torque given by Kushnir et al. (2017), an accurate, approximate, closed form for the dynamical tide in a highly eccentric MS-CO binary can be obtained. Contrary to existing models of dynamical tides (e.g. Vigna-Gómez et al. 2020), our formulation improves in accuracy as the binary eccentricity increases. We give closed forms for both the tidal torque and inspiral rate of such an MS-CO binary.

In Section 2, we review the relevant equations. In Sections 3 and 4, we derive accurate, approximate closed forms for the torque and energy transfer rate in the binary. In Section 5, we apply results to the binary radio pulsar J0045-7319. We conclude and discuss in Section 6.

2 SUMMARY OF RELEVANT WORK

2.1 Tidal Torque in Massive Stars

We first review the case where the MS-CO binary is circular. Let M_2 be the mass of the CO, a be the semimajor axis of the binary, and ω the orbital angular frequency of the binary. The tidal torque exerted on the star by the companion is (Kushnir et al. 2017):

$$\tau = \hat{\tau}(\omega)\,\mathrm{sgn}\left(1-\frac{2\Omega_\mathrm{s}}{\omega}\right)\left|1-\frac{2\Omega_\mathrm{s}}{\omega}\right|^{8/3}, \tag{1}$$

$$\begin{aligned}\hat{\tau}(\omega) &= \frac{GM_2^2 r_c^5}{a^6}\left(\frac{\omega}{\sqrt{GM_c/r_c^3}}\right)^{8/3}\left[\frac{r_c}{g_c}\left(\frac{\mathrm{d}N^2}{\mathrm{d}\ln r}\right)_{r=r_c}\right]^{-1/3}\\ &\quad\times\frac{\rho_c}{\bar{\rho}_c}\left(1-\frac{\rho_c}{\bar{\rho}_c}\right)^2\left[\frac{3}{2}\frac{3^{2/3}\Gamma^2(1/3)}{5\cdot 6^{4/3}}\frac{3}{4\pi}\alpha^2\right],\\ &\equiv \beta_2\frac{GM_2^2 r_c^5}{a^6}\left(\frac{\omega}{\sqrt{GM_c/r_c^3}}\right)^{8/3}\frac{\rho_c}{\bar{\rho}_c}\left(1-\frac{\rho_c}{\bar{\rho}_c}\right)^2.\end{aligned} \tag{2}$$

Here, Ω_s is the spin of the massive star, N is the Brünt-Vaisala frequency, r is the radial coordinate within the star, and r_c, M_c, g_c, ρ_c, $\bar{\rho}_c$ are the radius of the RCB, the mass contained within the convective core, the gravitational acceleration at the RCB, the stellar density at the RCB, and the average density of the convective core, respectively. α and β_2 are numerical constants defined by Kushnir et al. (2017), where $\beta_2 \approx 1$ is a good approximation for a large range of stellar models. In Eq. (1), we have written the terms such that $\hat{\tau}$ contains all the spin-independent terms.

© 2020 The Authors

2.2 Perturbation from an Eccentric Companion: Hansen Coefficients

Separately, we review the general procedure for calculating tidal dissipation due to an eccentric perturber. The gravitational potential of an eccentric companion can be decomposed at quadrupolar order as a sum over circular orbits (Storch & Lai 2013; Vick et al. 2017):

$$U = \sum_m U_{2m}(\vec{r}, t), \tag{3}$$

$$\begin{aligned} U_{2m}(\vec{r}) &= -\frac{GM_2 W_{2m} R^2}{D(t)^3} e^{-imf(t)} Y_{2m}(\theta, \phi), \\ &= -\frac{GM_2 W_{2m} R^2}{a^3} Y_{2m}(\theta, \phi) \sum_{N=-\infty}^{\infty} F_{Nm} e^{-iN\Omega t}, \end{aligned} \tag{4}$$

$$F_{Nm} = \frac{1}{\pi} \int_0^{\pi} \frac{\cos\left[N(E - e\sin E) - mf(E)\right]}{(1 - e\cos E)^2} \, \mathrm{d}E. \tag{5}$$

Here, R is the radius of the star, $W_{2\pm2} = \sqrt{3\pi/10}$, $W_{2\pm1} = 0$, $W_{20} = -\sqrt{\pi/5}$, $D(t)$ is the instantaneous distance between the star and companion, f is the true anomaly, Y_{lm} denote the spherical harmonics, and Ω is the mean motion of the companion. F_{Nm} denote are the *Hansen coefficients* for $l = 2$ (also denoted X^n_{2m} in Murray & Dermott 1999).

By considering the effect of each summand in Eq. (4), the total torque on the star, energy transfer in the inertial frame, and heating in the star's corotating frame can be obtained (Storch & Lai 2013; Vick et al. 2017):

$$\tau = \sum_{N=-\infty}^{\infty} F_{N2}^2 \hat{\tau}(\omega = N\Omega - 2\Omega_{\rm s}), \tag{6}$$

$$\begin{aligned} \dot{E}_{\rm in} = \frac{1}{2} \sum_{N=-\infty}^{\infty} \Bigg\{ &\left(\frac{W_{20}}{W_{22}}\right)^2 N\Omega F_{N0}^2 \hat{\tau}(\omega = N\Omega) \\ &+ N\Omega F_{N2}^2 \hat{\tau}(\omega = N\Omega - 2\Omega_{\rm s}) \Bigg\}, \end{aligned} \tag{7}$$

$$\dot{E}_{\rm rot} = \dot{E}_{\rm in} - \Omega_{\rm s}\tau, \tag{8}$$

where $\hat{\tau}(\omega)$ is the torque exerted by a perturber on a circular trajectory with orbital frequency ω. Our notation differs from that of Vick et al. (2017), where we write $\hat{\tau}(\omega) = T_0 \, \mathrm{sgn}(\omega)\hat{F}(|\omega|)$ in their notation, to easier incorporate the results of the previous section.

2.3 Objective of This Paper

The objective of this paper is to study the effect of dynamical tides in an eccentric MS-CO binary. First, we compute the tidal torque by substituting the torque due to a CO on a circular orbit [Eq. (1)] into the summation Eq. (6), obtaining

$$\tau = \sum_{N=-\infty}^{N=\infty} F_{N2}^2 \hat{\tau}(r_c) \mathrm{sgn}\left(N - \frac{2\Omega_{\rm s}}{\Omega}\right) \left| N - \frac{2\Omega_{\rm s}}{\Omega} \right|^{8/3}. \tag{9}$$

The energy transfer rate in the inertial frame is similarly obtained by substituting Eq. (1) into Eq. (7)

$$\begin{aligned} \dot{E}_{\rm in} = \frac{\hat{\tau}(r_c, \Omega)}{2} \sum_{N=-\infty}^{\infty} \Bigg[&N\Omega F_{N2}^2 \mathrm{sgn}(N - 2\Omega_{\rm s}/\Omega) \left| N - 2\Omega_{\rm s}/\Omega \right|^{8/3} \\ &+ \left(\frac{W_{20}}{W_{22}}\right)^2 \Omega F_{N0}^2 |N|^{11/3} \Bigg]. \end{aligned} \tag{10}$$

These two expressions give the spin synchronization timescale of the star as well as the inspiral time of the binary due to dynamical tides. While exact, these expressions are difficult to evaluate for larger eccentricities, where one often must sum hundreds or thousands of terms, each of which has a different F_{Nm}. In the subsequent sections, our objective is to obtain closed-form approximations to Eqs. (9–10).

3 APPROXIMATING HANSEN COEFFICIENTS

Recall that the Hansen coefficients are defined as the Fourier series coefficients of part of the companion's gravitational potential

$$\frac{a^3}{D(t)^3} e^{-imf} = \sum_{N=-\infty}^{\infty} F_{Nm} e^{-iN\Omega t}. \tag{11}$$

Observe that $F_{(-N)m} = F_{N(-m)}$, so we will only study the Hansen coefficient behavior for $m \geq 0$.

3.1 $m = 2$ Hansen Coefficient Behavior at High Eccentricity

We first consider the case where $m = 2$. We give an example of the behavior of the F_{N2} for $e = 0.9$ in Fig. 1, and make the following observations:

- F_{N2} is much larger for $N \geq 0$ than for $N < 0$.
- For $N \geq 0$, F_{N2} has only one substantial peak. The only characteristic scale for N is the pericenter harmonic

$$N_{\rm p} \equiv \lfloor \Omega_{\rm p}/\Omega \rfloor, \tag{12}$$

where $\Omega_{\rm p}$ is the pericenter frequency, defined by

$$\Omega_{\rm p} \equiv \Omega \frac{\sqrt{1+e}}{(1-e)^{3/2}}. \tag{13}$$

Thus, we expect that the peak of the F_{N2} should occur at $\sim N_{\rm p}$, which is indeed the case.

- Since the left hand side of Eq. (11) is smooth, the Fourier coefficients must fall off exponentially for $N \gg N_{\rm p}$ by the Paley-Wiener theorem.
- Since there are no characteristic timescales between Ω and $\Omega_{\rm p}$, we anticipate the Hansen coefficients must be scale free between $N = 1$ and $N_{\rm p}$, i.e. a power law.

Motivated by these considerations, we assume the Hansen coefficients can be approximated by

$$F_{N2} \approx \begin{cases} C_2 N^p e^{-N/\eta_2} & N \geq 0, \\ 0 & N < 0, \end{cases} \tag{14}$$

for some fitting coefficients C_2, p, and η_2. By performing fits to F_{N2}, we found that $p \approx 2$ is relatively constant for modest-to-large large eccentricities. This is expected, as the left hand side of Eq. (11) resembles the second derivative of a Dirac delta for $N \lesssim N_{\rm p}$ when the eccentricity is substantial[1]. For the remainder of this work, we take $p = 2$ to be fixed.

[1] Note that the left hand side of Eq. (11) is sharply peaked about $t = 0$, is periodic with period $P = 2\pi/\Omega$, and has zero derivative three times every period (at $t = \epsilon$, $t = P/2$, and $t = P - \epsilon$ for some small $\epsilon \sim 1/\Omega_{\rm p}$). This characteristics imply that it can be well approximated by the second derivative of a Gaussian with width $\sim 1/\Omega_{\rm p}$. For frequencies $\Omega \lesssim \Omega_{\rm p}$, this Gaussian is further well approximated by a Dirac delta, which has a flat Fourier transform ($\propto N^0$). Since time differentiation multiplies by N in frequency space, we see indeed that $F_{N2} \propto N^2$ for $N \lesssim N_{\rm p}$.

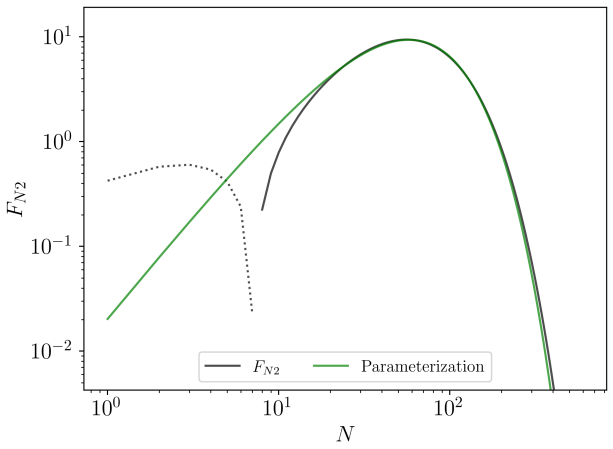

Figure 1. Plot of Hansen coefficients F_{N2} for $e = 0.9$, where dotted line denotes negative values. The green line is the parameterization of Eq. (14) with η_2 and C_2 given by Eqs. (17–18).

To constrain the remaining two free parameters η_2 and C_2 the normalization, we use the well known Hansen coefficient moments (Hut 1981)

$$\sum_{N=-\infty}^{\infty} F_{N2}^2 = \frac{1 + 3e^2 + 3e^4/8}{(1-e^2)^{9/2}} \equiv \frac{f_5}{(1-e^2)^{9/2}}, \tag{15}$$

$$\sum_{N=-\infty}^{\infty} F_{N2}^2 N = \frac{2}{(1-e^2)^6}\left(1 + \frac{15e^2}{2} + \frac{45e^4}{8} + \frac{5e^6}{16}\right) \equiv \frac{2f_2}{(1-e^2)^6}. \tag{16}$$

This fixes

$$\eta_2 = \frac{4f_2}{5f_5\,(1-e^2)^{3/2}}, \tag{17}$$

$$C_2^2\eta_2^5 = \frac{4f_5}{3\,(1-e^2)^{9/2}}. \tag{18}$$

This parameterization is compared to explicit evaluation of the Hansen coefficients in Fig. 1. The agreement is particularly striking as this parameterization uses zero free parameters.

3.2 $m = 0$ Hansen Coefficient Behavior at High Eccentricity

We now turn to the case where $m = 0$ in Eq. (11). These coefficients also only have one characteristic scale in harmonic space (N_p), but are also symmetric. Therefore, the natural ansatz is of form

$$F_{N0} = C_0 e^{-|N|/\eta_0}. \tag{19}$$

The two free parameters C_0 and η_0 are again constrained by the well known moments (Hut 1981)

$$\sum_{N=-\infty}^{\infty} F_{N0}^2 = \frac{f_5}{(1-e^2)^{9/2}}, \tag{20}$$

$$\sum_{N=-\infty}^{\infty} F_{N0}^2 N^2 = \frac{9e^2}{2\,(1-e^2)^{15/2}} f_3. \tag{21}$$

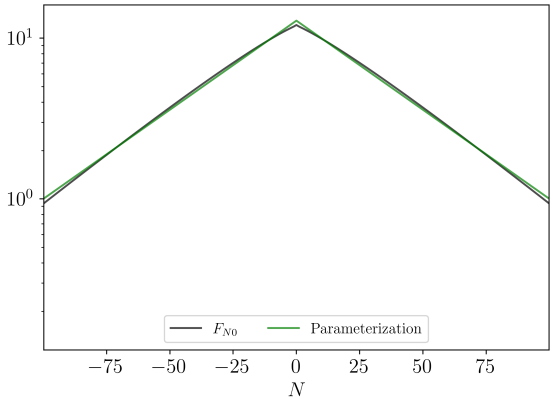

Figure 2. Plot of F_{N0} for $e = 0.9$. The green line denotes the parameterization of Eq. (19) with η_0 and C_0 given by Eqs. (22–23).

This fixes

$$\eta_0^2 = \frac{9e^2 f_3}{(1-e^2)^3 f_5}, \tag{22}$$

$$C_0^2\eta_0 = \frac{f_5}{(1-e^2)^{9/2}}. \tag{23}$$

4 EVALUATING TORQUE AND ENERGY TRANSFER

We now return to the summations in Section 2.3 and simplify them using the parameterized Hansen coefficients from the previous section.

4.1 Tidal Torque

We return now to Eq. (9). By replacing the F_{N2} with the approximation Eq. (14) and replacing the sum with an integral, we obtain

$$\tau = \hat{\tau}\int_0^\infty C_2^2 N^4 e^{-2N/\eta_2}\,\mathrm{sgn}\,(N - 2\Omega_\mathrm{s}/\Omega)\,|N - 2\Omega_\mathrm{s}/\Omega|^{8/3}\,\mathrm{d}N. \tag{24}$$

This can be further simplified. Define $N_\mathrm{max} = 10\eta_2/3$ to be the N for which the integrand in Eq. (24) is maximized if $\Omega_\mathrm{s} = 0$ (if Ω_s is large, the integrand is maximized at $N = 2\eta_2 \simeq N_\mathrm{max}$). We first consider the high-spin limit where $|\Omega_\mathrm{s}| \gg N_\mathrm{max}\Omega/2$. In this limit, Eq. (9) can be evaluated directly with the known Hansen coefficient moments, which gives

$$\lim_{\Omega_\mathrm{s}\to\infty} \tau = -\hat{\tau}\,\mathrm{sgn}(\Omega_\mathrm{s})\;|2\Omega_\mathrm{s}/\Omega|^{8/3}\,\frac{f_5}{(1-e^2)^{9/2}}. \tag{25}$$

Next, we consider the low-to-moderate spin regime $2\Omega_\mathrm{s}/\Omega \lesssim N_\mathrm{max}$. To accommodate for moderate spins, we assume that $N - 2\Omega_\mathrm{s}/\Omega$ can be approximated by

$$N - 2\Omega_\mathrm{s}/\Omega \simeq \frac{N}{N_\mathrm{max}}\left(N_\mathrm{max} - \frac{2\gamma_\tau\Omega_\mathrm{s}}{\Omega}\right), \tag{26}$$

for some free parameter γ_τ. Using this prescription, Eq. (24) can

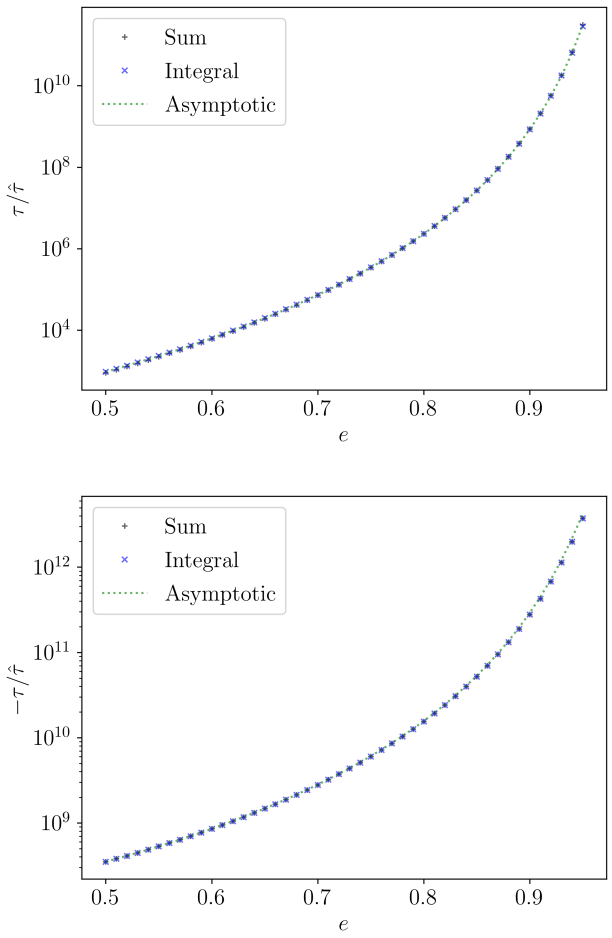

Figure 3. Tidal torque on a non-rotating (top) and rapidly rotating ($\Omega_s/\Omega = 400$; bottom) star with a companion having orbital eccentricity e. Blue plus signs represent explicit summation of Eq. (9), blue crosses are evaluated using the integral approximation Eq. (24), and the green dashed line is Eq. (27).

be integrated analytically, since $\int_0^\infty x^p e^{-x}\,\mathrm{d}x = \Gamma(p-1)$[2]. After integrating, γ_τ is constrained by requiring our expression reproduce the high spin limit [Eq. (25)] when taking $|\Omega_s| \to \infty$. Then, the torque becomes

$$\tau = \hat{\tau}\frac{f_5(\eta_2/2)^{8/3}}{(1-e^2)^{9/2}}\,\mathrm{sgn}\left(1-\gamma_\tau\frac{\Omega_s}{\eta_2\Omega}\right)\left|1-\gamma_\tau\frac{\Omega_s}{\eta_2\Omega}\right|^{8/3}\frac{\Gamma(23/3)}{4!}, \tag{27}$$

$$\gamma_\tau = 4\left(\frac{4!}{\Gamma(23/3)}\right)^{3/8} \approx 0.691. \tag{28}$$

See Figs. 3 and 4 for the accuracy of this prediction. As expected from the construction of this approximation, both the low and high spin limits are well captured, and the scaling for intermediate spins is also somewhat accurate.

[2] The key to the success of our approach is that sums of form $\sum_{n=-\infty}^{\infty} F_{N2}^2 N^p$ can be evaluated for non-integer p in terms of Γ, which is not possible with the traditional techniques used to evaluate these sums for integer p.

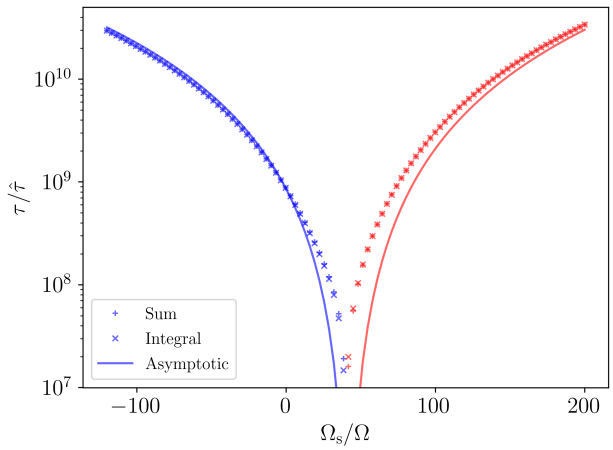

Figure 4. Tidal torque as a function of spin for a highly eccentric $e = 0.9$ companion. Pluses represent direct summation of Hansen coefficients, crosses represent the integral approximation, and solid lines represent the analytic closed form. Blue [red] means positive [negative] torque on the star.

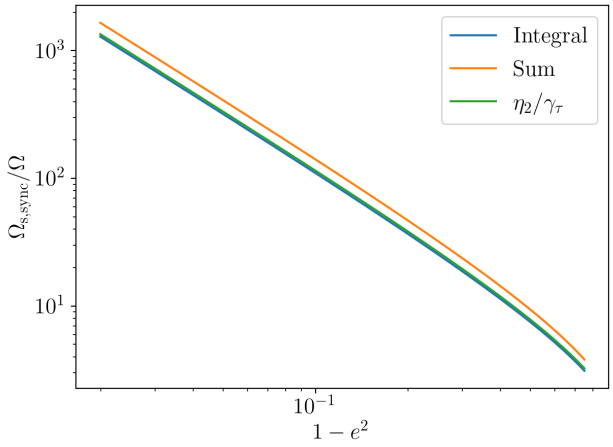

Figure 5. Pseudosynchronization frequency. Integral form is obtained by performing root finding using the integral form for the torque. We see that Eq. (29) is a very good approximation.

4.2 Pseudosynchronization

Eq. (27) shows that there is a single Ω_s for which the torque τ vanishes. This is the pseudosynchronization spin frequency, given by

$$\frac{\Omega_{s,ps}}{\Omega} = \frac{\eta_2}{\gamma_\tau} = \frac{4f_2}{5\gamma_\tau f_5\left(1-e^2\right)^{3/2}}. \tag{29}$$

This has the expected scaling $\Omega_{s,ps} \propto (1-e^2)^{-3/2}$, but is more accurate than $\Omega_{s,ps} \simeq \Omega_p$, as seen in Fig. 5. By comparison, in standard weak friction theory of equilibrium tides, the pseudo-synchronized rotation rate is given by (Alexander 1973; Hut 1981)

$$\frac{\Omega_{s,ps}^{(Eq)}}{\Omega} = \frac{f_2}{f_5\left(1-e^2\right)^{3/2}}. \tag{30}$$

This differs from our Eq. (29) by a factor of 1.15.

Note that, very near the pseudosynchronized spin frequency,

Eq. (27) predicts that $d\tau/d\Omega_s \approx 0$. This is inaccurate and is an artifact of our factorization ansatz in Eq. (33).

4.3 Closed Form for Energy Transfer

We now simplify Eq. (7) and replace F_{N2} and F_{N0} with their approximations Eqs. (14, 19) to obtain

$$\dot{E}_{\rm in} = \frac{\hat{\tau}\Omega}{2}\int_0^\infty \left[C_2^2 N^5 e^{-2N/\eta_2}\,{\rm sgn}\,(N-2\Omega_s/\Omega)\,|N-2\Omega_s/\Omega|^{8/3} + 2\left(\frac{W_{20}}{W_{22}}\right)^2 C_0^2 e^{-2N/\eta_0} N^{11/3}\right] dN. \quad (31)$$

We evaluate the $m = 2$ and $m = 0$ components of this expression separately.

We first examine the $m = 2$ contribution using a very similar procedure to what we used for the torque. Again, we define $N_{\rm max} = 23\eta_2/6$ the N for which the integrand is maximized. The high spin limit $\Omega_s \gg N_{\rm max}\Omega/2$ comes out to be

$$\lim_{\Omega_s\to\infty} \dot{E}_{\rm in}^{(m=2)} = -\frac{\hat{\tau}\Omega}{2}\,{\rm sgn}(\Omega_s)|2\Omega_s/\Omega|^{8/3}\frac{2f_2}{(1-e^2)^6}. \quad (32)$$

We then consider the low-to-moderate spin limit and factorize

$$N - 2\Omega_s/\Omega \simeq \frac{N}{N_{\rm max}}\left(N_{\rm max} - \frac{2\gamma_E\Omega_s}{\Omega}\right), \quad (33)$$

where γ_E is a free parameter. This lets us integrate Eq. (31) analytically, and we can constrain γ_E by requiring the integral agree with Eq. (32). We obtain that

$$\dot{E}_{\rm in}^{(m=2)} = -\frac{\hat{\tau}\Omega f_5(\eta_2/2)^{11/3}}{2(1-e^2)^{9/2}}\frac{\Gamma(26/3)}{4!} \times {\rm sgn}\left(1-\gamma_E\frac{\Omega_s}{\eta_2\Omega}\right)\left|1-\gamma_E\frac{\Omega_s}{\eta_2\Omega}\right|^{8/3}, \quad (34)$$

$$\gamma_E = \left(\frac{5!2^{16/3}}{\Gamma(26/3)}\right)^{3/8} \approx 0.5886. \quad (35)$$

The $m = 0$ contribution to Eq. (31) is much more straightforward and can be directly integrated using the parameterization Eq. (19). We finally obtain the total energy transfer rate

$$\dot{E}_{\rm in} = -\frac{\hat{\tau}\Omega}{2}\left[\frac{f_5(\eta_2/2)^{11/3}}{(1-e^2)^{9/2}}\frac{\Gamma(26/3)}{4!} \times {\rm sgn}\left(1-\gamma_E\frac{\Omega_s}{\eta_2\Omega}\right)\left|1-\gamma_E\frac{\Omega_s}{\eta_2\Omega}\right|^{8/3} + \frac{f_5\Gamma(14/3)}{(1-e^2)^{10}}\left(\frac{3}{2}\right)^{8/3}\left(\frac{e^2 f_3}{f_5}\right)^{11/6}\right]. \quad (36)$$

We make plots in the two Ω_s regimes as a function of eccentricity in Fig. 6 and 7. Agreement is good again.

5 EXAMPLE SYSTEM: PSR J0045+7319

As an example of our calculations above, we consider PSR J0045-7319 binary system (Bell et al. 1995). The system was initially reported to have pulsar mass $M_2 = 1.4M_\odot$, $q = 6.3$, $e = 0.808$, orbital period $P = 51.17$ days, and $\dot{P} = -3.03\times10^{-7}$ (Kaspi et al. 1996). This gives a mass of $8.8M_\odot$ for the massive star.

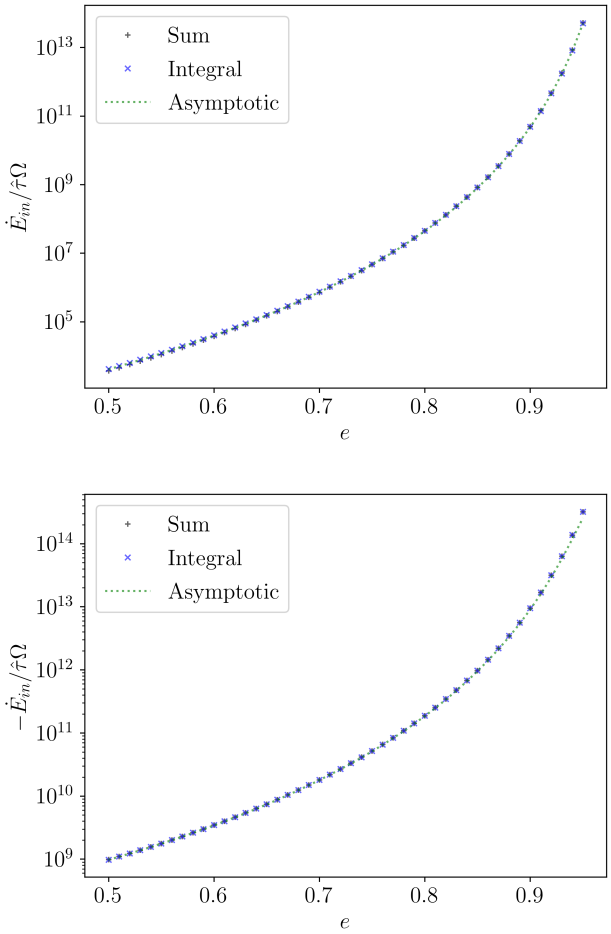

Figure 6. Plot of $\dot{E}_{\rm in}$ for a non-rotating (top) and rapidly rotating ($\Omega_s/\Omega = 400$; bottom) star. Blue pluses represent explicit summation of the Hansen coefficients, crosses the integral form Eq. (31), and the green dashed line the closed form Eq. (36).

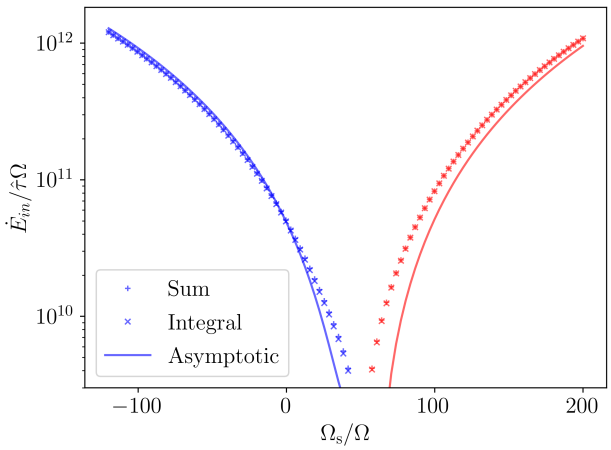

Figure 7. $\dot{E}_{\rm in}$ as a function of spin for a highly eccentric $e = 0.9$ companion. Pluses represent direct summation of Hansen coefficients, crosses represent the integral approximation, and solid lines represent the analytic closed form. Blue [red] means positive [negative] energy transfer into the stellar spin.

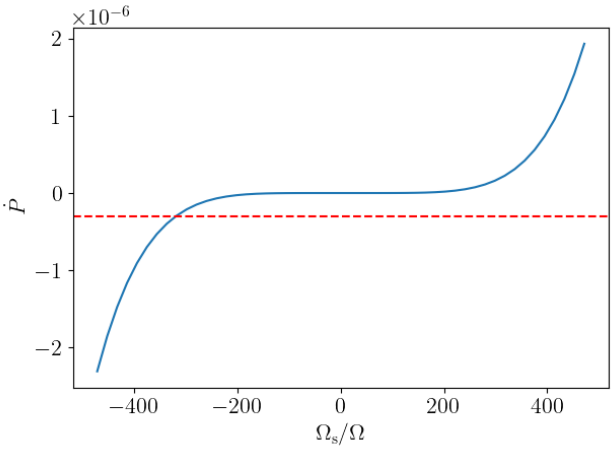

Figure 8. $\dot{P}$ as a function of Ω_s for the canonical parameters for J0045-7319, as evaluated by Eq. (36). The measured $\dot{P} = -3.03 \times 10^{-7}$ is shown by the horizontal red dashed line.

5.1 Spin of the Massive Star: Using Literature Values?

From these system parameters, we can also calculate the orbital separation $a = 126R_\odot$. The internal structure of the star can be obtained by comparison to detailed stellar structure calculations, and yield $M_c \approx 3M_\odot$ and $r_c \approx 1.38R_\odot$ (Kumar & Quataert 1998). With these parameters, the spin of the massive star can be computed using our calculations above. For simplicity, define

$$g\,(e, \Omega_s/\Omega) = -\frac{\dot{E}_{\rm in}}{\hat{\tau}\Omega}. \tag{37}$$

Then, by conservation of energy, $\dot{E}_{\rm in} + \dot{E}_g = 0$, where $\dot{E}_g$ is the change in the gravitational binding energy, given by

$$\dot{E}_g = \frac{GqM_2^2}{3a}\frac{\dot{P}}{P}. \tag{38}$$

To relate $g\,(e, \Omega_s/\Omega)$ to $\dot{P}$, we need to make assumptions about the ratio $\rho_c/\bar{\rho}_c$, which can only be obtained via stellar structure simulations. We take $\rho_c/\bar{\rho}_c \approx 1/3$ as a fiducial value. Fig. 8 then shows $\dot{P}$ as a function of Ω_s, using Eq. (36), where the measured $\dot{P}$ is shown by the horizontal red dashed line. It is clear that substantial retrograde rotation is necessary to match the observed $\dot{P}$.

5.2 Caveats

We can arrive at an upper bound for the $\dot{P}$ by setting the spin frequency equal to the breakup frequency. Then, taking the correct parameters and evaluating $\dot{E}_{\rm in}$, we obtain

$$\dot{P} \lesssim -\frac{6\pi}{q}\beta_2\left(\frac{r_c}{a}\right)^5\frac{\rho_c}{\bar{\rho}_c}\left(1-\frac{\rho_c}{\bar{\rho}_c}\right)^2 2^{8/3}\frac{f_2}{(1-e^2)^6}. \tag{39}$$

This comes out to be $r_c \gtrsim 1.16R_\odot$ for J0045+7319 when using $\rho_c/\bar{\rho}_c = 0.74$.

5.3 Stellar Structure Simulations

In previous literature, the primary star was initially taken to have $M_1 = 8.8M_\odot$ (Kumar & Quataert 1998; Lai 1996), by taking $M_2 \simeq 1.4M_\odot$ characteristic mass for NSs and multiplying by the observed q. A later, but still very old, study proposed $M_1 \approx 10M_\odot$ by comparison with stellar models. Using MESA to generate updated stellar models (TODO all citations), we compute an updated M_1 estimate, giving detailed stellar structure measurements.

At the level of approximation of this paper, our procedure is as follows: we use a few different values of convective overshooting and mixing, and metallicities, and compute stellar structures for both both non-rotating and highly rotating $\sim 0.95\Omega_{s,c}$ stars. We find that, in general, to match the observed T, L we must let the star evolve to $\sim 80\%$ of the way to complete core hydrogen depletion. We then sample a range of stellar masses, and find the stellar mass that best reproduces the observed T, L.

For all of these systems, $r_c \lesssim R_\odot$, in tension with our bound above.

6 CONCLUSION AND DISCUSSION

The primary results of the paper is Eq. (27), shown in Figs. 3 and 4 to be accurate across a range of spins and eccentricities. The energy dissipation rate is also computed using similar techniques and show good agreement (see Figs. 6 and 7).

- Thanks to some references (Barker & Ogilvie, my work), there seems to be some evidence that hydrodynamic wave breaking could cause all IGW to break and not reflect, once the pericenter wave reaches nonlinear amplitudes.
- As noted in the text, the approximate forms enforce $d\tau/d\Omega_s = 0$, which the actual torque does not satisfy. This introduces some slight errors in the exact value of the torque very near pseudosynchronization.

7 ACKNOWLEDGEMENTS

We thank Michelle Vick and Christopher O'Connor for fruitful discussions. YS is supported by the NASA FINESST grant 19-ASTRO19-0041.

REFERENCES

Alexander M., 1973, Astrophysics and Space Science, 23, 459
Bell J., Bessell M., Stappers B., Bailes M., Kaspi V., 1995, The Astrophysical Journal Letters, 447, L117
Goldreich P., Nicholson P. D., 1989, Astrophysical Journal, 342, 1079
Hurley J. R., Tout C. A., Pols O. R., 2002, Monthly Notices of the Royal Astronomical Society, 329, 897
Hut P., 1981, Astronomy and Astrophysics, 99, 126
Kaspi V., Bailes M., Manchester R., Stappers B., Bell J., 1996, Nature, 381, 584
Kumar P., Quataert E. J., 1998, The Astrophysical Journal, 493, 412
Kushnir D., Zaldarriaga M., Kollmeier J. A., Waldman R., 2017, Monthly Notices of the Royal Astronomical Society, 467, 2146
Lai D., 1996, The Astrophysical Journal Letters, 466, L35
Murray C. D., Dermott S. F., 1999, Solar system dynamics. Cambridge university press
Savonije G., Papaloizou J., 1983, Monthly Notices of the Royal Astronomical Society, 203, 581
Storch N. I., Lai D., 2013, Monthly Notices of the Royal Astronomical Society, 438, 1526
Vick M., Lai D., Fuller J., 2017, Monthly Notices of the Royal Astronomical Society, 468, 2296
Vigna-Gómez A., MacLeod M., Neijssel C. J., Broekgaarden F. S., Justham S., Howitt G., de Mink S. E., Mandel I., 2020, arXiv preprint arXiv:2001.09829

Zahn J.-P., 1975, Astronomy and Astrophysics, 41, 329

This paper has been typeset from a TEX/LATEX file prepared by the author.